International Global Navigation Satellite Systems Society
IGNSS Symposium 2015

Outrigger Gold Coast, Qld Australia
14-16 July, 2015

Range Error Analysis of TDOA Based UWB-IR Indoor Positioning System

Lian Zhang
School of Electrical and Electronic Engineering
Nanyang Technological University
Singapore
(+65) 90597619
lzhang025@e.ntu.edu.sg

Yanjia Luo
School of Electrical and Electronic Engineering
Nanyang Technological University
Singapore
luoy0012@ntu.edu.sg

Choi Look Law
School of Electrical and Electronic Engineering
Nanyang Technological University
Singapore
(+65) 67905424
ecllaw@ntu.edu.sg

ABSTRACT

The excellent performance of ultra-wideband impulse radio (UWB-IR) technology in indoor localization system has attracted increasing attention. As of today, most previous works focus on theoretical evaluation of the capabilities of UWB technology based on simplified simulations. The objective of this paper is to analyze how practically measured range using time-difference-of-arrival (TDOA) based UWB-IR positioning system deviates from the actual distance when the signal transmitter is located at various distances from the receiver. Empirical data of distances from 1m up to 35m are collected at INFINITUS lab, Nanyang Technological University, Singapore. A threshold-based estimator is used to compute the distance of flight. By investigating the mean and root mean square error (RMSE) of the estimated range, one constraint of indoor localization performance is found to be due to multipath propagation. Bias error is observed and is attributed to the front-end circuit delay due to near far signals. The study of range error suggests a more effective way to refine the position estimation algorithm and thus enhances the reliability of indoor localization technology.

KEYWORDS: time-difference-of-arrival (TDOA), ultra-wideband (UWB), indoor localization, multipath propagation, range error

1. INTRODUCTION

The extensive utilization of Global Positioning System (GPS) technology has effectively solved many real-life problems such as vehicle guidance, disaster rescue operation and missile targeting. Its accuracy of several meters satisfies the requirement of outdoor localization. However, in the era of Internet-of-Things (IoT), with the emerging demand for more intelligent ways to locate and control assets and people remotely, the performance of positioning technology is facing great challenges in complex indoor scenarios with dense multipath components (Gezici *et al*., 2005).

One of the most prospective candidates is UWB-IR technology. Compared to conventional narrowband systems, UWB-IR stands out for its high accuracy, wide frequency range, low power consumption and low cost. The large bandwidth of UWB impulse radio (>500MHz) guarantees a high time-of-arrival (TOA) resolution, improving the accuracy to centimeter level. The deviation of the estimated coordinate from the real location is mainly attributed to four sources: multipath propagation, multiple-access interference, obstructed LOS propagation and timing imperfections (Sahinoglu *et al.,* 2008).

This project aims to investigate the dependency of range error on the distance between signal transmitter and receiver, and correlations with the above mentioned impairments in indoor environment. To obtain the geolocation of the target transmitter, information about the first arriving pulse at the receiver ends is needed. Intensive research has been undertaken focusing on this area. The time-of-arrival points can be estimated coherently by analysing the correlation between the received signal waveform and the expected signal pattern based on a priori knowledge about the signal, such as matched filtering (MF), or non-coherently by comparing the detected signal energy with a threshold (Guvenc *et al*., 2006) (Reggiani and Maggio, 2005). As MF method requires the received signal to be non-distorted, the low-cost sub-Nyquist sampling rate deployed in daily applications can hardly satisfy this condition.

This paper emphasizes on the study of the threshold energy detection approach. A UWB-IR indoor positioning system is used to collect raw data. Rather than directly utilizing the TOA information to calculate the range, which might lead to clock drift error by unsynchronized transmitter and receiver nodes, TDOA method is chosen (Xia *et al*., 2010). This study provides valuable insights into the factors that constrain the localization accuracy and hence helps refine the position estimation algorithm.

The rest of this paper is organized as follows. Part 2 explains the apparatus and procedures conducted in the experiment. Part 3 provides an overview of the positioning algorithm and the derivation of the estimation method. Part 4 presents the results on mean and RMSE of the estimated range and the performance analysis of different distances. Part 5 concludes the paper.

2. EXPERIMENTAL METHODOLOGY

2.1 Experimental Setup

In this experiment, a battery-powered tag (Figure 1) driven by Texas Instrument MSP430 low power microcontroller is used to transmit UWB signal pulses at a frequency of 3.25MHz (±10ppm). The signal received by the two sensors (Rx_1 and Rx_2) travels through polyethylene Unshielded Twisted Pair (UTP) Cat6 cables (with dielectric permittivity of 2.25) to reach the

locator box (Figure 2), which converts the RF band signal to baseband signal, filters off out-of-band interferences, amplifies and detects the envelope of the UWB-IR signals. The digitized data is then transmitted to a computer through a USB2.0 interface and processed using MATLAB® (Figure 3) (Law, 2014). The tag and sensors are mounted at height of 1.2m from the ground.

Figure 1. UWB-IR Tag

Figure 2. Sensor & Locator Box

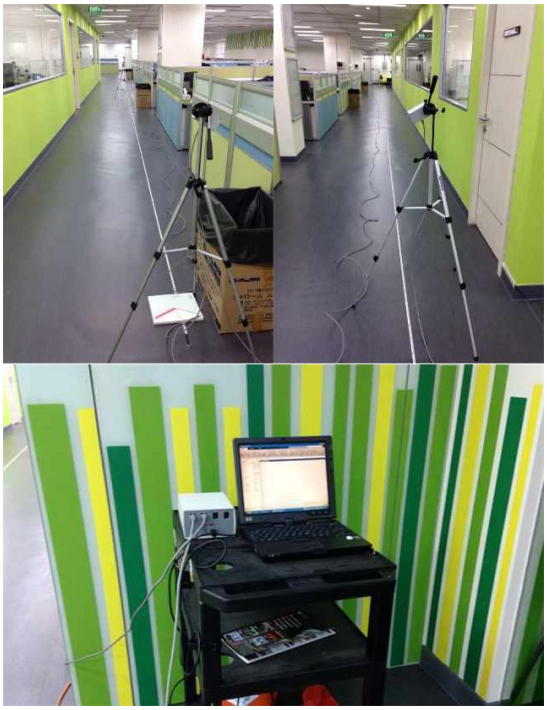

Figure 3. Measurement Environment & Experimental Setup

2.2 Procedure

1) Separate Rx_1 and Rx_2 by 1m.

2) Place the tag on Rx_1.

3) Collect 500 frames (each frame consists of 16,000 discrete time points with a sampling interval of 0.08906ns) of sample data of the signal received by Rx_1 and Rx_2 respectively.

4) Move the tag to Rx_2.

5) Repeat step 3).

6) Change the distance between Rx_1 and Rx_2 from 1m to 2m, 3m…35m and repeat steps 2) ~ 5) for each distance.

7) Process the collected data to analyze the relationship between range error and tag-sensor distance using MATLAB® codes.

3. ALGORITHM

After the raw data is collected, the leading edge of each received pulse is detected to be the time-of-arrival (TOA) of the signal. By manipulating the time-difference-of-arrival (TDOA) between Rx_1 and Rx_2, the range can be estimated.

3.1 TOA Detection

The method of iterative threshold selection is used to detect the leading edge of the received UWB pulses. The initial threshold is set to be 0.05 times the maximum amplitude and the periods of signal lower than the threshold are turned off. The value is incremented by 0.05 times the maximum amplitude repetitively until the signal-off periods reach a quarter of the frame length. The final threshold is checked to be lower than the mean amplitude of the 16,000 points.

An integration window is then chosen by comparing the intervals between consecutive signal-off points. The energy sum is computed starting from each signal-off point over the integration window and is weighted according to the duration between this point and the next signal-off point. Peaks with the weighted energy exceeding 0.9 of the maximum energy are selected as TOA points.

3.2 TDOA

Consider the case when the tag is placed at Rx_1, TOA at Rx_1 is:

$$TRx_{11} = Tx_1 + t_{1d1} + tc_1 \qquad (1)$$

where Tx_1 is the signal generation time from the tag at Rx_1, t_{1d1} is the front-end circuit delay time of Rx_1 with the tag at Rx_1, and tc_1 is the cable delay at Rx_1.

TOA at Rx_2 is:

$$TRx_{21} = Tx_1 + t_{12} + t_{2d1} + tc_2 \qquad (2)$$

where t_{12} is the time of flight from Rx_1 (tag) to Rx_2 in air, t_{2d1} is the front-end circuit delay time of Rx_2 with the tag at Rx_1, and tc_2 is the cable delay at Rx_2.

Assume $t_{1d1} = t_{2d1}$, subtract (2) by (1):

$$TDOA_{21} = TRx_{21} - TRx_{11} = t_{12} + (tc_2 - tc_1). \qquad (3)$$

Consider the tag placed at Rx_2, TDOA can be obtained similarly:

$$TDOA_{12} = TRx_{12} - TRx_{22} = t_{12} + (tc_1 - tc_2). \qquad (4)$$

3.3 Range Estimation

Add (3) and (4), then divide by 2, the time of flight in the air is:

$$t_{12} = (TDOA_{21} + TDOA_{12})/2.$$

Note that t_{12} is obtained by equivalent time sampling at ADC of the locator box. The sampling interval, t_{samp}, is approximately 0.08906ns. Thus the real time distance between Rx_1 and Rx_2 is:

$$d_{12} = c * t_{12} * t_{samp} \qquad (5)$$

where c is the speed of electromagnetic wave propagation in free space.

4. RESULTS AND DISCUSSION

4.1 TOA Detection

Figure 4 & 5 capture the selected threshold and detected TOA at Rx_1 when the tag is placed at Rx_1 using the method of iterative threshold selection. At 1m, the approximated threshold is around 0.25 whereas the threshold is selected to be 0.4 at 8m. The sharpest point (when value of TOA trace jumps from 0 to 1) of the leading edge is considered as the time-of-arrival (TOA) of the UWB pulse.

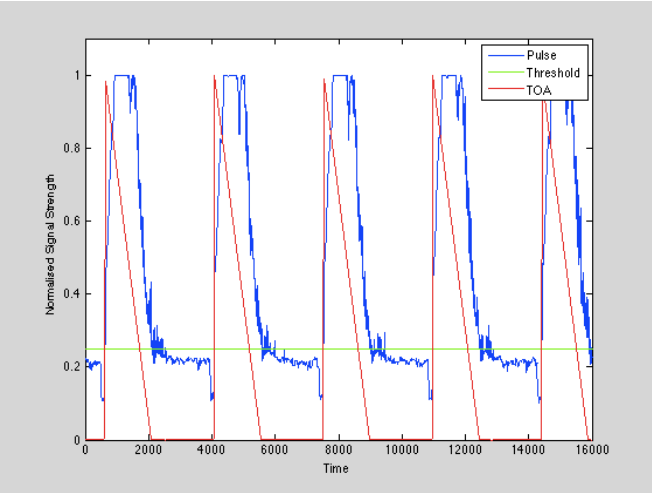

Figure 4. Screen Capture of TOA at Rx_1 at 1m

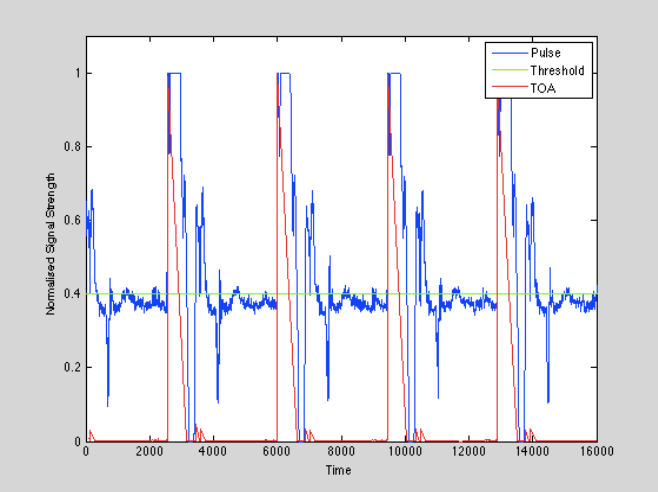

Figure 5. Screen Capture of TOA at Rx_1 at 8m

4.2 TDOA Distribution

Figure 6 & 7 below show the TDOA distribution of the 500 frames of data at 7m, with each frame having 4~5 TOA values. $TDOA_{21}$ corresponds to the case where the tag is placed at Rx_1 while $TDOA_{12}$ corresponds to Rx_2. Both graphs form a Gaussian distribution.

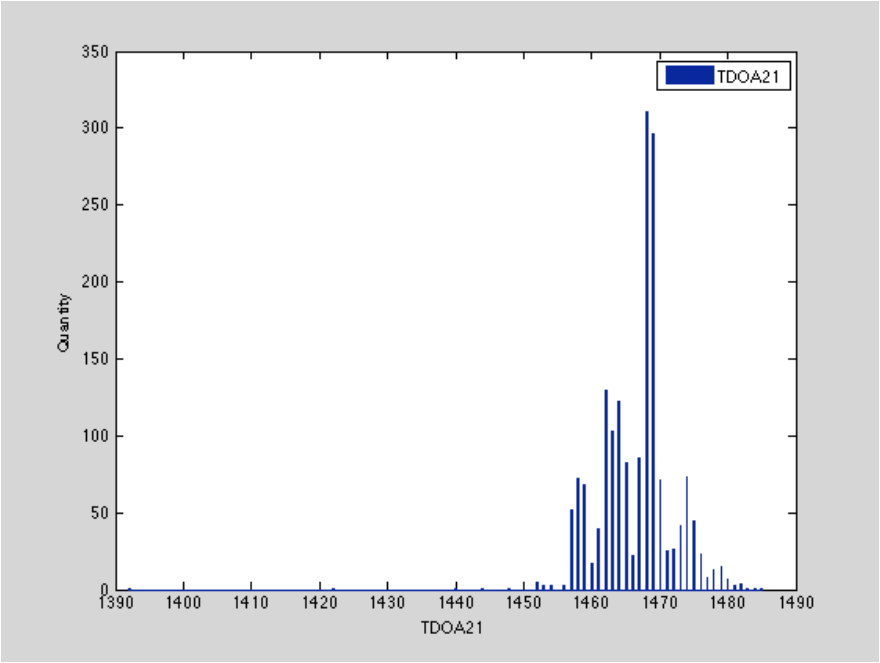

Figure 6. $TDOA_{21}$ Distribution at 7m

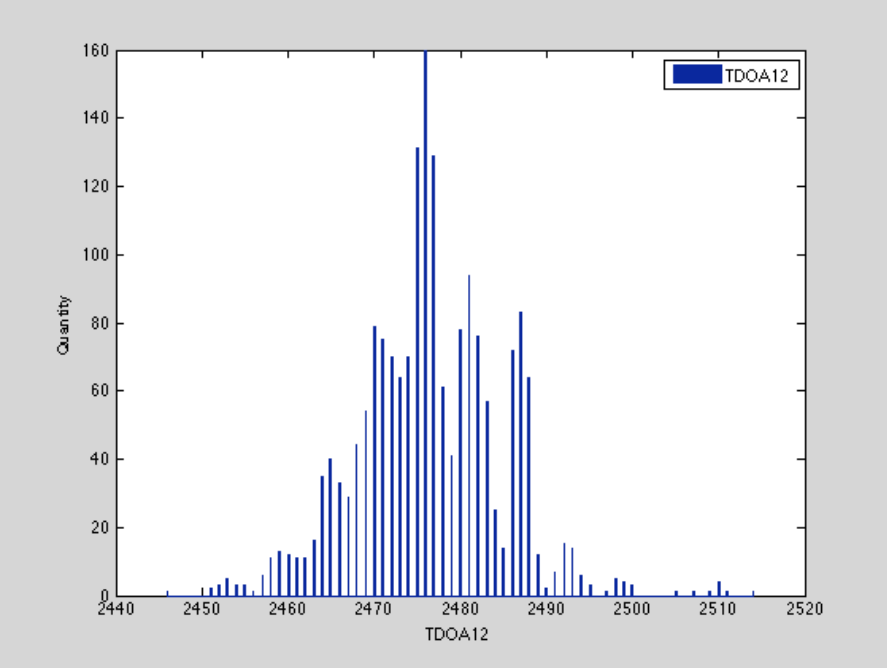

Figure 7. $TDOA_{12}$ Distribution at 7m

4.3 Range Distribution

Substituting the TDOA values obtained from 4.2 into (5), the range between Rx_1 and Rx_2 can be calculated. Examples of the estimated range distribution from the 500 samples at 7m and 24m are shown in Figure 8 & 9. Both graphs form a Gaussian distribution.

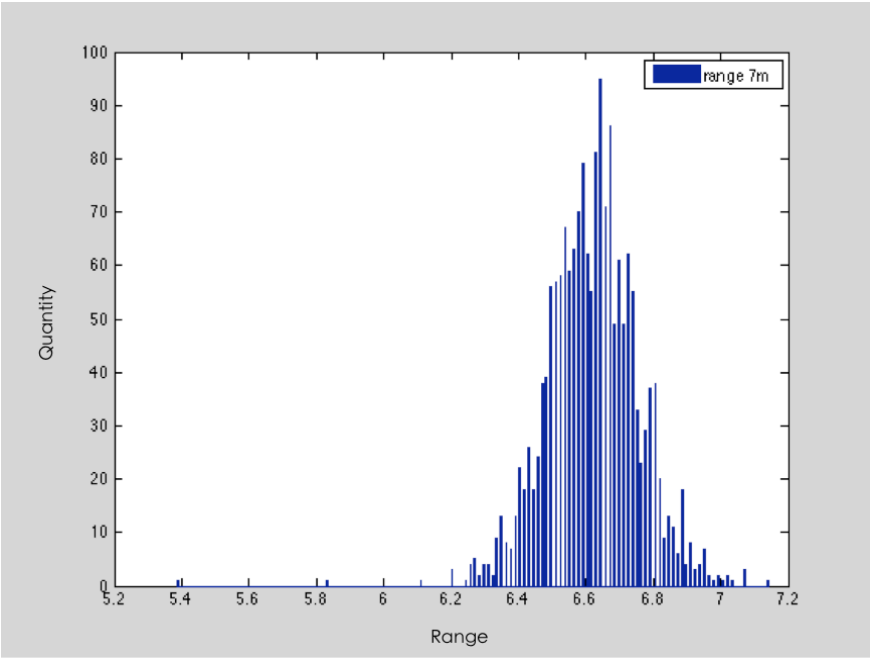

Figure 8. Range Distribution at 7m

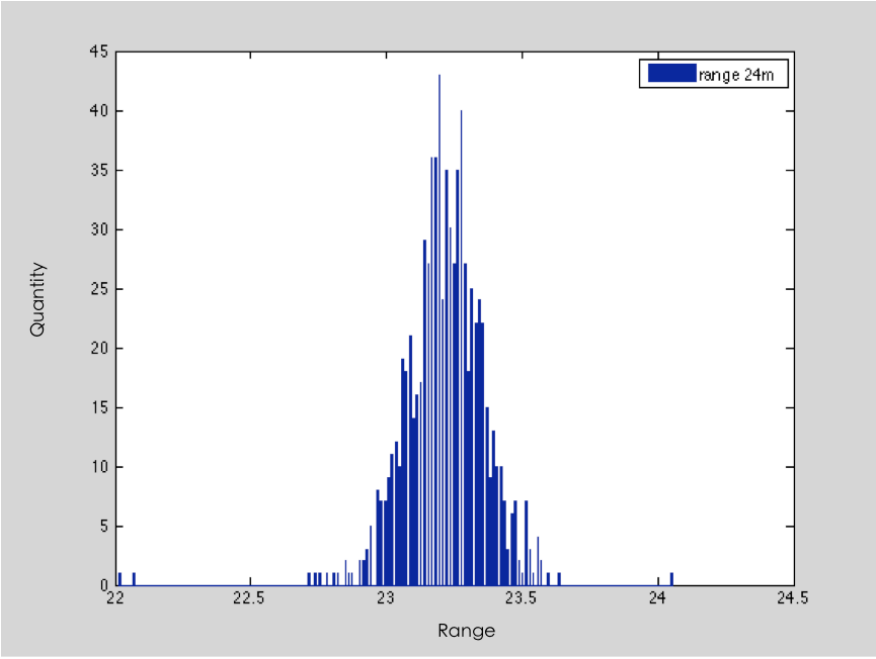

Figure 9. Range Distribution at 24m

The mean of the estimated range out of the 500 samples as well as its standard deviation (RMSE) from 1m to 35m are tabulated in Table 1 and plotted in Figure 10.

Distance [m]	1	2	3	4	5	6	7	8	9	10	11	12	13
Mean [m]	0.30	1.45	1.99	2.36	4.03	4.05	6.62	7.72	7.71	8.37	9.06	11.2	10.6
RMSE [m]	0.09	0.09	0.18	0.13	0.17	0.14	0.13	0.13	0.18	0.22	0.18	0.21	0.18

Distance [m]	14	15	16	17	18	19	20	21	22	23	24	25	26
Mean [m]	12.6	13.1	14.4	15.7	16.2	18.0	18.0	18.9	20.2	21.3	23.2	24.1	25.2
RMSE [m]	0.16	0.20	0.18	0.20	0.16	0.35	0.16	0.13	0.12	0.32	0.15	1.19	0.14

Distance [m]	27	28	29	30	31	32	33	34	35
Mean [m]	26.3	26.7	27.9	26.6	31.6	33.1	33.3	38.5	33.7
RMSE [m]	0.14	0.40	0.33	8.27	0.18	0.68	3.20	12.26	0.48

Table 1. Mean Range and RMSE from 1m to 35m

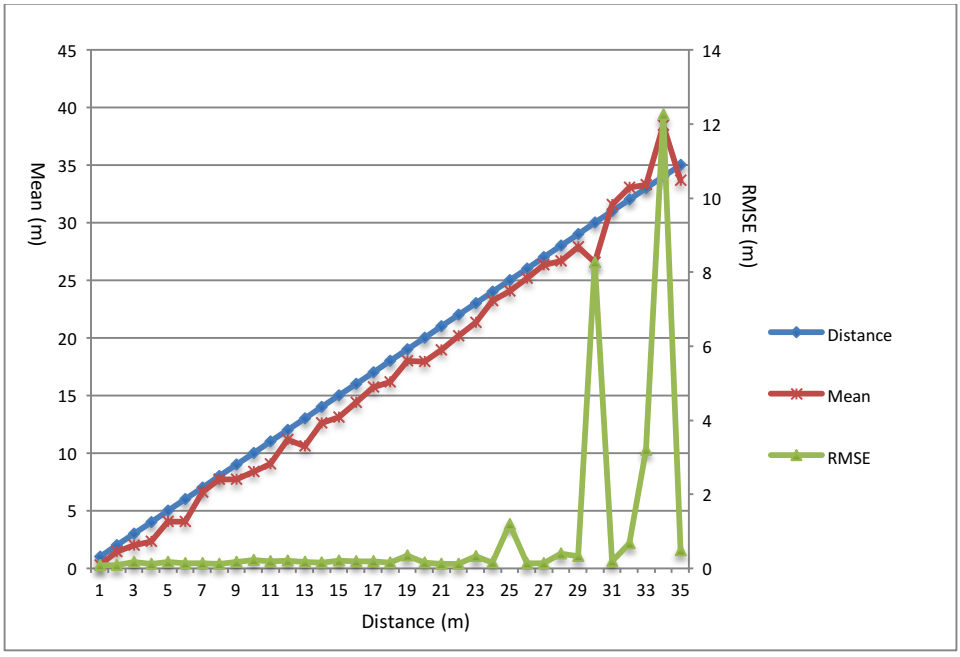

Figure 10. Plot of Mean Range and RMSE from 1m to 35m

Both the table and graph show that the mean range deviates from the actual distance by around 1.03m. The error becomes significant when exceeding 30m. The standard deviation (RMSE) is around 0.20m below 30m and the received signal becomes unstable at larger distances, which is due to power attenuation and multipath propagation. These result in the less accurate mean range estimation after 30m.

Although the large bandwidth of UWB makes the signal highly resolvable, the inter-pulse interference due to multipath propagation should still be taken into account in fast-pulse systems. In our case, the floor and ceiling of INFINITUS lab are made of re-enforced concrete with metal grids for high loads. In the process of propagation, part of the signal which hits the floor/ceiling is absorbed while the remaining attenuated part is reflected and reaches the receiver nodes later (Popa, 2002).

Figure 11 below shows the simplified scenario of our lab. The vertical distance between the ceiling and the floor is 3m. Rx_1 and Rx_2 are 1.2m high. Consider the case of the tag being placed at Rx_1. The signal generated by the tag can either reach Rx_2 directly (L1) or be reflected by the floor/ceiling first and then reach Rx_2 (L2).

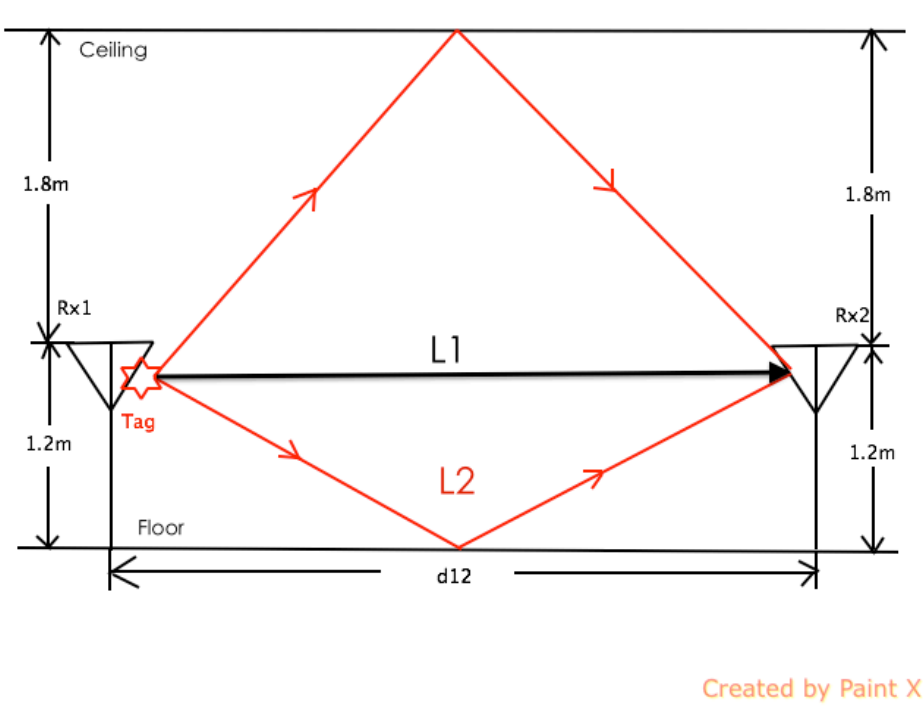

Figure 11. Simplified Scenario of INFINITUS Lab

When d_{12} = 2m,
$L2 - L1 = 2*\sqrt{(1.2^2 + 1^2)} - 2 = 1.124$m.

The number of time points between the two received pulses is:
$1.124/ (c * t_{samp}) = 42.07$.

When d_{12} = 30m,
$L2 - L1 = 2*\sqrt{(1.2^2 + 15^2)} - 30 = 0.0958$m.

The number of time points between the two received pulses is:
$0.0958/ (c * t_{samp}) = 3.587$.

As can be seen, the direct pulse leads the reflected pulse by about 42 time points at 2m, which can be easily differentiated in the waveform. As the distance increases, the TOA difference between the two paths becomes smaller. At 30m, the two pulses reach the receiver almost at the same time. Above 30m, pulses travelling by diverse paths may overlap with each other and

it would be even harder to differentiate them. The mixture of signals could decrease the sharpness of the leading edges of the received pulses and degrade the time resolution.

Besides, as the distance increases, multipath propagation is more likely to take place due to a more complex environment involved. The amplification of the original signal by the superposition of the indirect path signals as well as noise would affect the threshold selection process. Hence failure to detect the sharpest point of the first arriving pulse as TOA contributes to the range error. Therefore the indoor positioning performance deteriorates at larger distances (Dardari, 2008) (Alavi, 2006).

Another observation is that the estimated range at most distance points shows a lower value than the actual distance. In 3.2, we assumed that $t_{1d1} = t_{2d1}$, i.e. the front-end circuit delay time at Rx_1 and Rx_2 are equal. However, this is not true since the signal magnitude received by Rx_1 and Rx_2 are different with the tag being placed at each receiver. To examine the reliability of the results, the front-end circuit delay is analysed.

4.4 Front-end Circuit Delay Analysis

Since $t_{1d1} \neq t_{2d1}$ and $t_{1d2} \neq t_{2d2}$, (3) and (4) are amended as:
$TDOA_{21} = TRx_{21} - TRx_{11} = t_{12} + (tc_2 - tc_1) + (t_{2d1} - t_{1d1})$.
$TDOA_{12} = TRx_{12} - TRx_{22} = t_{12} + (tc_1 - tc_2) + (t_{1d2} - t_{2d2})$.

Hence,

$$t_{2d1} - t_{1d1} = TDOA_{21} - t_{12} - (tc_2 - tc_1); \quad (6)$$
$$t_{1d2} - t_{2d2} = TDOA_{12} - t_{12} + (tc_2 - tc_1). \quad (7)$$

Thus,

$$t_{12} = (TDOA_{21} + TDOA_{12})/2 - (t_{2d1} - t_{1d1})/2 - (t_{1d2} - t_{2d2})/2. \quad (8)$$

The length of the cable connecting the locator box and Rx_1 is physically measured to be 8.81m, whereas the cable connecting with Rx_2 is 30.07m. Thus,
$tc_2 - tc_1 = (30.07m - 8.81m)/ (t_{samp}*c/2.25^{1/2})$,
where $c/2.25^{1/2}$ is the speed of electromagnetic wave propagation in the UTP cable.

The time of flight from Rx_1 to Rx_2 in time points, t_{12}, can be substituted by: $d_{12}/(t_{samp}*c)$, where d_{12} is the actual distance between Rx_1 and Rx_2 while c is the speed of electromagnetic wave propagation in free space.

Using $TDOA_{21}$ and $TDOA_{12}$ obtained from 4.2, the front-end circuit delay in time points is calculated from (6) and (7). The results are tabulated in Table 2 and plotted in Figure 12~14.

Distance [m]	1	2	3	4	5	6	7	8
t2d1-t1d1 [time points]	-134	-127	-137	-152	-136	-171	11.0	10.0
t1d2-t2d2 [time points]	81.7	86.4	61.0	29.6	63.7	24.8	-39.8	-34.5
Sum [time points]	-52.3	-40.6	-76.0	-122	-72.3	-146	-28.8	-24.5

Distance [m]	9	10	11	12	13	14	15	16
t2d1-t1d1 [time points]	-56.6	-92.5	-92.1	-87.0	-116	-130	-132	-106
t1d2-t2d2 [time points]	-40.3	-30.3	-53.8	24.4	-64.5	26.3	-10.4	-13.8
Sum [time points]	-96.9	-123	-146	-62.6	-181	-104	-142	-120

Distance [m]	17	18	19	20	21	22	23	24
t2d1-t1d1 [time points]	-127	-123	-115	-129	-130	-107	-104	-108
t1d2-t2d2 [time points]	30.1	-14.9	39.0	-25.1	-26.2	-28.5	-21.5	47.6
Sum [time points]	-96.9	-138	-76.0	-154	-156	-136	-126	-60.4

Distance [m]	25	26	27	28	29	30	31	32
t2d1-t1d1 [time points]	-113	-128	-123	-116	-125	-118	-12.8	-23.7
t1d2-t2d2 [time points]	41.1	66.7	71.1	16.5	41.0	-139	52.6	99.6
Sum [time points]	-71.9	-61.3	-51.9	-99.5	-84.0	-257	39.8	75.9

Distance [m]	33	34	35
t2d1-t1d1 [time points]	-95.5	-108	-124
t1d2-t2d2 [time points]	115	441	24.1
Sum [time points]	19.5	333	-99.9

Table 2. Front-end Circuit Delay from 1m to 35m

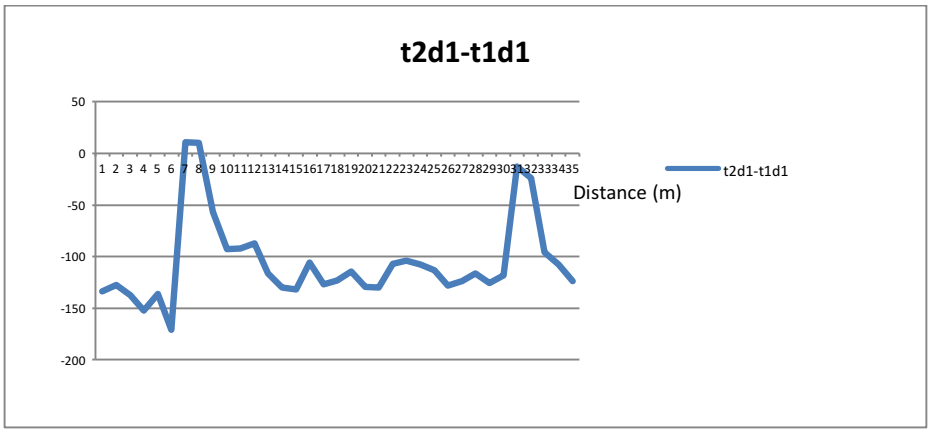

Figure 12. Front-end Circuit Delay Plot 1

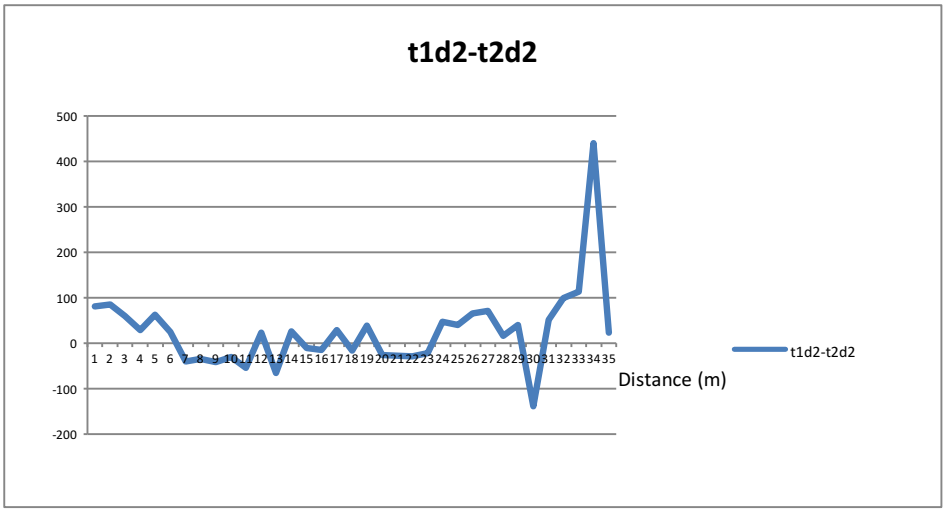

Figure 13. Front-end Circuit Delay Plot 2

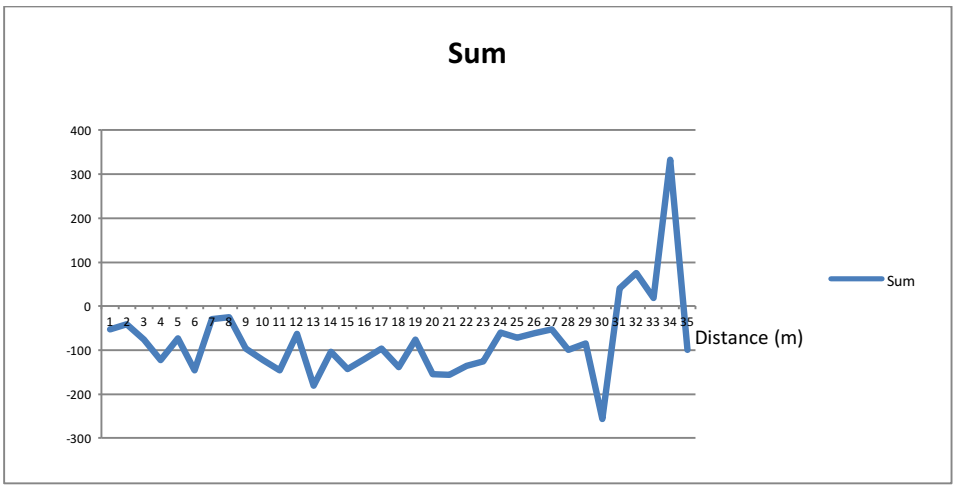

Figure 14. Front-end Circuit Delay Plot 3

From the table and plots above, the sum of (t_{2d1}-t_{1d1}) and (t_{1d2}-t_{2d2}) is negative when the distance is less than 30m. According to (8), the estimated t_{12} in 3.3 should be smaller than the actual time of flight. Thus the calculated range d_{12} is smaller than the actual distance between the tag and sensor, which agrees with the results obtained in 4.3.

5. CONCLUSIONS

The excellent performance of UWB technology facilitates various civil and military applications. Nevertheless, its accuracy is constrained within a certain range in cluttered indoor areas. In this paper, the analysis of UWB range error dependency through practical measurement covering 1~35m shows that longer distances between the signal transmitter and receiver would largely degrade the positioning accuracy due to multipath propagation. Also the study has proved that the negative range bias is attributed to the front-end circuit delay. The

robustness of future UWB-IR indoor localization system will depend on the complexity level of the indoor scenario and how precisely the positioning algorithm can detect the first leading edge of the received signal travelling through long distances.

ACKNOWLEDGEMENTS

We wish to acknowledge the funding support for this project from Nanyang Technological University under the Undergraduate Research Experience on Campus (URECA) program.

REFERENCES

Alavi B, Pahlavan K (2006) Modeling of the TOA-based distance measurement error using UWB indoor radio measurements, *Communications Letters, IEEE* , vol.10, no.4, pp.275,277

Dardari D, Chong CC, Win MZ (2008) Threshold-Based Time-of-Arrival Estimators in UWB Dense Multipath Channels, *Communications, IEEE Transactions on* , vol.56, no.8, pp.1366,1378

Gezici S, Zhi T, Giannakis GB, Kobayashi H, Molisch AF, Poor HV, Sahinoglu Z (2005) Localization via ultra-wideband radios: a look at positioning aspects for future sensor networks, *Signal Processing Magazine, IEEE* , vol.22, no.4, pp.70,84

Global Positioning System (2014) *Wikipedia, the free encyclopedia.* Retrieved May 16, 2014, from http://en.wikipedia.org/wiki/Global_Positioning_System

Guvenc I, Sahinoglu Z, Orlik PV (2006) TOA estimation for IR-UWB systems with different transceiver types, *IEEE Trans. on Microwave Theory and Techniques*, vol. 54, no. 4, pp.1876-1886

Law CL (2014) Portable low-power IR-UWB system, *Internet of Things (WF-IoT), 2014 IEEE World Forum on* , vol., no., pp.474,478

Popa A (2002) *Re: Which materials block radio waves the most (and why)?* Retrieved from http://www.madsci.org/posts/archives/2002-03/1015162213.Eg.r.html

Reggiani L, Maggio GM (2005) Rapid search algorithms for code acquisition in UWB impulse radio communications, *IEEE J. Sel. Areas Commun.,* vol. 23, no. 5, pp. 898–908.

Sahinoglu Z, Gezici S, Guvenc I (2008) *Ultra-wideband Positioning Systems: Theoretical Limits, Ranging Algorithms, and Protocol,* Cambridge University Press

Xia J, Law CL, Zhou Y, Koh KS (2010) 3–5 GHz UWB Impulse Radio Transmitter and Receiver MMIC Optimized for Long Range Precision Wireless Sensor Networks, *Microwave Theory and Techniques, IEEE Transactions on* , vol.58, no.12, pp.4040,4051